
Article:
Sparkes, J. orcid.org/0000-0002-1961-1384 and Holland, C. orcid.org/0000-0003-0913-2221 (2018) The energy requirements for flow-induced solidification of silk. Macromolecular Bioscience. 1800229. ISSN 1616-5187

https://doi.org/10.1002/mabi.201800229

DOI: 10.1002/mabi.((insert number))

Article Type: Communication

The energy requirements for flow induced solidification of silk[a]

James Sparkes and Chris Holland*

Mr. J. Sparkes

Natural Materials Group, Department of Materials Science and Engineering, Sir Robert Hadfield Building, Mappin Street, Sheffield, S1 3JD, UK.

Email: jesparkes1@sheffield.ac.uk

Dr. C. Holland.

Natural Materials Group, Department of Materials Science and Engineering, Sir Robert Hadfield Building, Mappin Street, Sheffield, S1 3JD, UK.

Email: christopher.holland@sheffield.ac.uk

Natural silk spinning has undergone strong selection for resource efficiency and thus presents a biomimetic ideal for fibre production. Industrial replication of natural silk fibres would enable access to low energy, cost efficient processing, but is hampered by a lack of understanding surrounding the conversion of liquid feedstock into a solid fibre as a result of flow. Previously, shear stress, shear rate or time have been presented as criteria for silk fibre formation, but here

[a] **Supporting Information** is available online from the Wiley Online Library or from the author.

we propose that spinning requires carefully balancing all three, and is a result of controlled energy accumulation in the feedstock. To support this hypothesis, rheology is used to probe the energy required for conversion, compare differences between amorphous solid and ordered fibre production and explain the energetic penalty the latter demands. New definitions of what constitutes an artificial silk fibre are discussed, along with methods to ensure that each spinning criterion is met during biomimetic spinning.

1 Introduction

Emulating the process of natural silk spinning is a long held aim in the field of biomaterials, as unfettered access to silk's attractive properties would provide huge commercial benefits arising from efficient continuous fibre production, without the hindrances associated with traditional production methods.[1]

While spider silk is perhaps the most well-known, or at least promoted, super material, the vast majority of everyday silk products are woven from fibres produced from cocoons spun as a protective layer by the Chinese silkworm Bombyx mori. In their native environment, B. mori spin, via pultrusion,[2] a dual filament fibre composed primarily of the protein fibroin,[3] coated in layers of a secondary protein known as sericin, which acts as a lubricant in the duct[4] and a binder[5,6] in the cocoon, a non-woven composite structure.[7] Whilst *B. mori's* natural fibre mechanical properties[8] are less desirable than those of, say the dragline filaments of Nephila edulis,[9] there is abundant evidence to suggest that they can be further processed to comparable performance levels[10–12] and their generally more abundant, accessible nature makes them currently a more practical technology platform.[13–19]

The majority of studies have explored various aspects of spinning fibroins, opting to focus on recombinant feedstock production,[20,21] die design,[22–27] fibre spinning, the mechanical properties of natural and artificially spun fibres, and post processing methods that can be undertaken in order to improve initial mechanical properties.[28–30] Our previous work has supplemented these industrially relevant methods at a more fundamental level by exploring the flow properties of silk protein feedstocks,[4,31–37] and how these relate to the aforementioned aspects of spinning.

The criterion for silk fibre formation, i.e. solidification through gelation, has been much debated in the literature, with successive studies putting forward evidence for gelation as a product of how hard (stress), how fast (rate), or how long (time) the sample is sheared. Here we propose a new approach, which seeks to combine all three, suggesting that fibroin gelation occurs due to energy accumulation. We describe this in terms of work per unit volume, expressed as a function of shear stress, shear rate and time.[38–40] To demonstrate this, we subject fibroin samples to steady shear until gelation and assess the total work done to reach this point. In doing so we identify a threshold for gelation which remains relatively constant, despite variation in material properties.[41] We consider these results within the wider context of understanding the fundamental mechanisms behind shear induced denaturation alongside the implications for industrialists wishing to mimic silk fibre spinning, as it allows for much less stringent conditions in feedstock production.

2 Experimental Section

2.1 Sample preparation

Native silk fibroin feedstock was extracted (using our previously described method[34]) from the glands of Bombyx mori silkworms in the wandering stage without any further preparation before testing. Fibroin concentration was assessed by drying out the portion of the gland next to that used for rheology and given as dry weight percent.

2.2 Rheological characterisation

All Rheological tests were conducted on a Bohlin Gemini Rheometer (Malvern Instruments, UK) at constant temperature and humidity, with a cone and plate geometry (10 mm diameter, 1° cone, 30 µm truncation) used to ensure a constant shear rate in the sample. After loading, a sheath of low viscosity fluid (water) was created around the sample to avoid dehydration and subsequent skinning effects in the pre-test environment.[34]

The pre-test procedures began with 100 s of steady shear (1 s^{-1}) to ensure homogeneous sample distribution, with apparent viscosity noted as the mean viscosity recorded from the final 30 s. A low strain (0.02) oscillatory sweep across a range of frequencies (25 – 0.1 Hz) was used to ensure that the sample remained fluid, before the main tests were run. Samples were grouped on the basis of their apparent viscosity η_1 in 500 Pa.s intervals and subjected to an extended period of steady shear at a rate between 3 and 15 s^{-1}, chosen to ensure a wide range of shear rates was considered.

Determination of the shear rate dependent viscosity $\eta(\gamma)$ was assessed through the assumption that the well-known Cox-Merz relation[42] is valid for fibroin, which means that $\eta(\gamma)$ is well approximated by $|\eta^*(\omega)|$. Application of the simplified Carreau-Yasuda model:

$$\eta(\dot{\gamma}) = \eta_0(1 + (\lambda\dot{\gamma})^a)^{\frac{n-1}{a}} \qquad (1)$$

To this data yields values for the zero shear viscosity η_0, along with the longest relaxation time (λ), lower critical shear rate ($\dot{\gamma}_{LC}$), and both the rate (a) and severity of shear thinning (n). Goodness of fit was gauged via Escudier's method,[43] while model validity was assessed by its ability to correctly predict the apparent (η_1) and test (η_τ) viscosities.

Oscillatory data was superimposed onto a master curve in order to assess the consistency of both the batch, and the experimental method. Higher rate steady shear data was curtailed beyond the time where a rapid rise in both viscosity and normal force were observed. Since the viscosity under steady shear was observed to transition from an initially high viscosity (η_α) to a lower, steady, final viscosity (η_β) as a function of time ($\eta(t)$) it seemed appropriate to fit a model which is numerically equivalent to the full Carreau-Yasuda model:

$$\eta(t) = \eta_\beta + \left(\eta_\alpha - \eta_\beta\right)\left(1 + (\tau t)^c\right)^{\frac{d-1}{c}} \quad (2)$$

Where c and d describe the breadth and rate of the transition respectively. Goodness of fit was again assessed using Escudier's method.[43] Evaluation of total work done to the system was undertaken on a per unit volume basis using the methods first espoused by Janeschitz-Kriegl et al.,[38] which states that the work applied in a test of length t_β can be determined as:

$$w = \int_0^{t_\beta} \eta(t)\ \dot{\gamma}^2\, dt \quad (3)$$

Rearranging this to account for the fact that in our case, shear rate is constant, and that the shear stress, rather than viscosity, is the measured value, results in the following definite integral which is readily summed using the trapezoid rule.

$$w = \dot{\gamma} \int_0^{t_\beta} \sigma(t)\, dt \quad (4)$$

This analysis was applied to both the apparent and test viscosity data to determine the total work done to each sample.

2.2.1 Statistical Analysis and data availability

Unless otherwise stated, data is presented as mean ± standard deviation from n repeats, with significance determined using unpaired t-tests with $P<0.0001$. The full data set is availably freely online at http://dx.doi.org/ 10.15131/shef.data.6464858.

3 Results and Discussion

3.1 Oscillatory and low rate steady shear response

The initial set of rheological tests confirmed that the fibroin samples tested were representative of a typical B. mori feedstock and therefore suitable for characterisation of their work to gelation (**Figure 1**). Specifically, the application of low rate steady shear provides a homogeneous starting point for further testing and allows estimation of the zero shear viscosity when combined with the oscillatory sweep response (**Figure 1a,b)**. Concentration determination shows the spread typical of fibroin (**Figure S1)**, with the expected lack of correlation with viscosity (**Figure S1, inset**). The combinatorial pre-test confirms the use of a typical fibroin feedstock which was unaffected by the extraction and loading procedures, before principal testing commences.

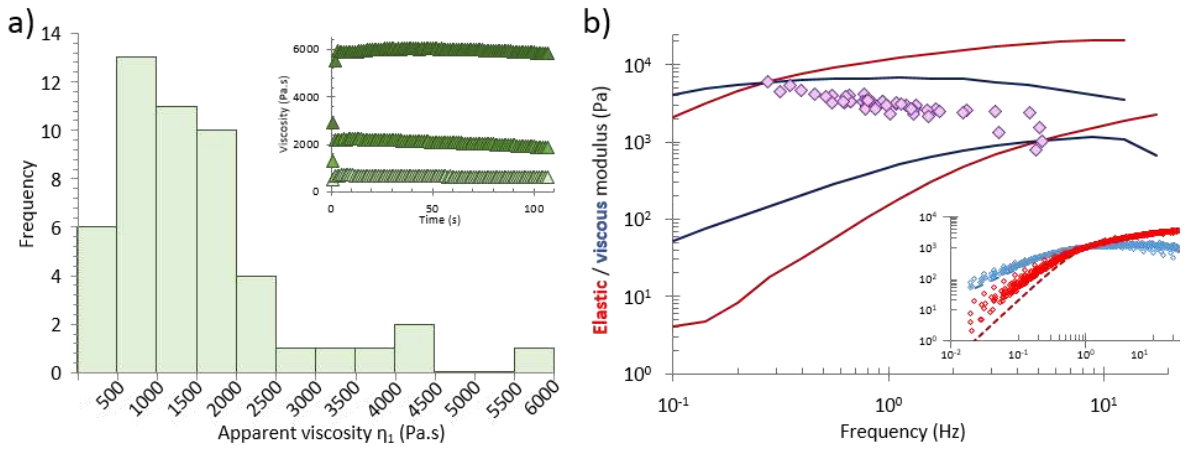

Figure 1– Preliminary testing. (a) Apparent viscosity distribution: The spread of apparent viscosities tested are shown in 500 Pa.s increments. Mean apparent viscosity is 1524 ± 1166 Pa.s (n=50), slightly lower than Laity's[34] 2015 result. **(Inset) - Low rate steady shear response:** exemplar responses of fibroin samples with **high**, **medium**, and **low** apparent viscosities highlight the behaviour, which shows the typical stress overshoot, followed by a slight reduction to a plateau viscosity η_1. **(b) Fibroin's oscillatory response:** In sample variation is shown by plotting the **crossover point** (frequency where **elastic** and **viscous** moduli

are equal), with the moduli of the most and least elastic samples also plotted across the entire frequency range in order to better illustrate the range of responses. **(Inset)** Close similarity in the superposition of oscillatory sweeps with frequency and modulus normalised against the crossover point shows consistency between samples. Allowing us to treat the normalised data as repeated sweeps of a generic fibroin sample which can be fitted with a binary Maxwell model (dotted lines).

The Cox-Merz relation allows for the extraction of data equivalent to destructive test results such as that gleaned from shear ramps, without the need to perform said experiment, providing us with insight into how silk compares to typical synthetic polymers.[44] To this end, oscillatory data fitted well using the simplified Carreau-Yasuda model (R^2 = 0.999), with model parameters n and λ showing good correlation with zero shear viscosity (**Figure S2**), while the third (a), which describes the breadth of transition to shear-thinning behaviour, is less clearly linked.

The degree to which native silk feedstocks match these models is largely predicated on the assumption that they behave like polymer melts under flow. However, whilst the small strain, elastic deformation of oscilaltory tests is useful, it does not replicate all the aspects and material response to actual plastic deformation that occurs during steady shear flow. Therefore it is imperative that these models are tested and validated before further use, and as such, the use of steady shear data provides a useful tool to probe the response of silk to deformation.

Comparing the measured viscosity at low shear (1 s^{-1}) with that predicted by the relevant converted oscillatory response data shows excellent agreement between the two techniques (**Figure 2, inset i**) and anchors the Cox-Merz generalisation for silk under low flow conditions.

However, application of the same model at higher rates (**Figure 2, inset ii**) shows a considerable under-representation of the extent of shear thinning and hence over-estimates the viscosity by a considerable margin. Hence the Cox-Merz generalisation is most suited to determining the zero shear viscosity of silk samples and as a result new approaches and interpretations will be required to predict the properties of silk under higher shear rates (i.e. the aquamelt hypothesis[44]).

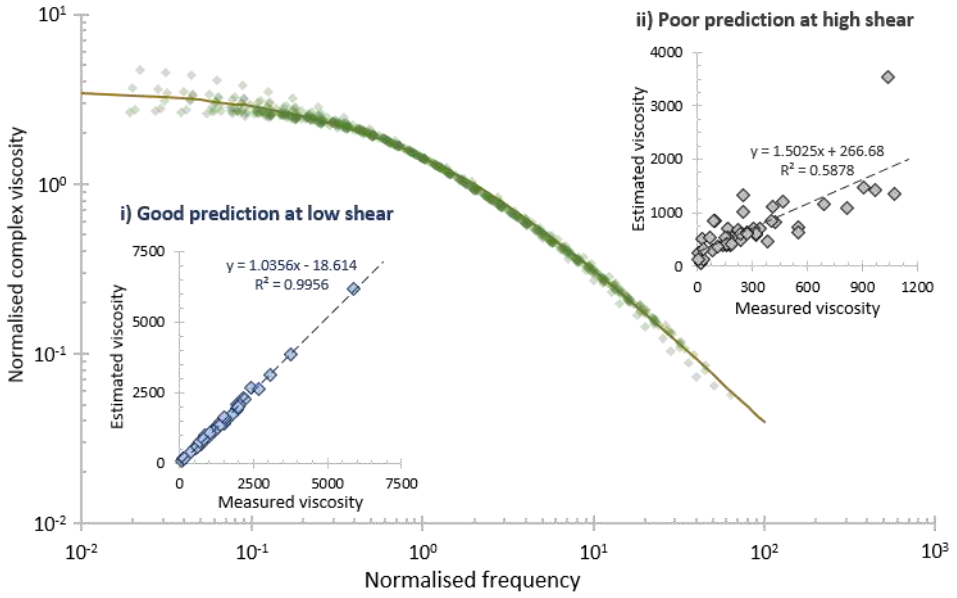

Figure 2 - Oscillatory –shear equivalence. Normalised **complex viscosity** data (against crossover), again fitted with **a simplified Carreau-Yasuda model**. **(Insets)** Relation between measured apparent viscosity (η_1, η_τ), and that predicted by the Cox-Merz relation at corresponding **low (i)** and **high (ii)** shear rates.

3.2 High rate steady shear response

Assessment of the work required for gelation for samples at higher rates of shear allows for some interesting observations. From an experimental perspective perhaps the most important is the time required to reach an equilibrium viscosity (i.e. flow response) under steady shear, with length scales far in excess of that assumed in typical shear rate ramps,[4,31–36,45] meaning that

there is a far greater dependence on rates of change than previously assumed (**Supporting Information note 1**).

Looking to the total work input required to induce gelation, as defined at the point by which the material changes from shear thinning to shear thickening,[46] when considered in isolation, high shear work to gelation results cluster around an average value of 2.75±1.37 $J.g^{-1}$ (n=44), or with the inclusion of the work done at low shear rates as a result of pre-shearing of the sample at 2.90±1.43 $J.g^{-1}$ (**Figure 3**).

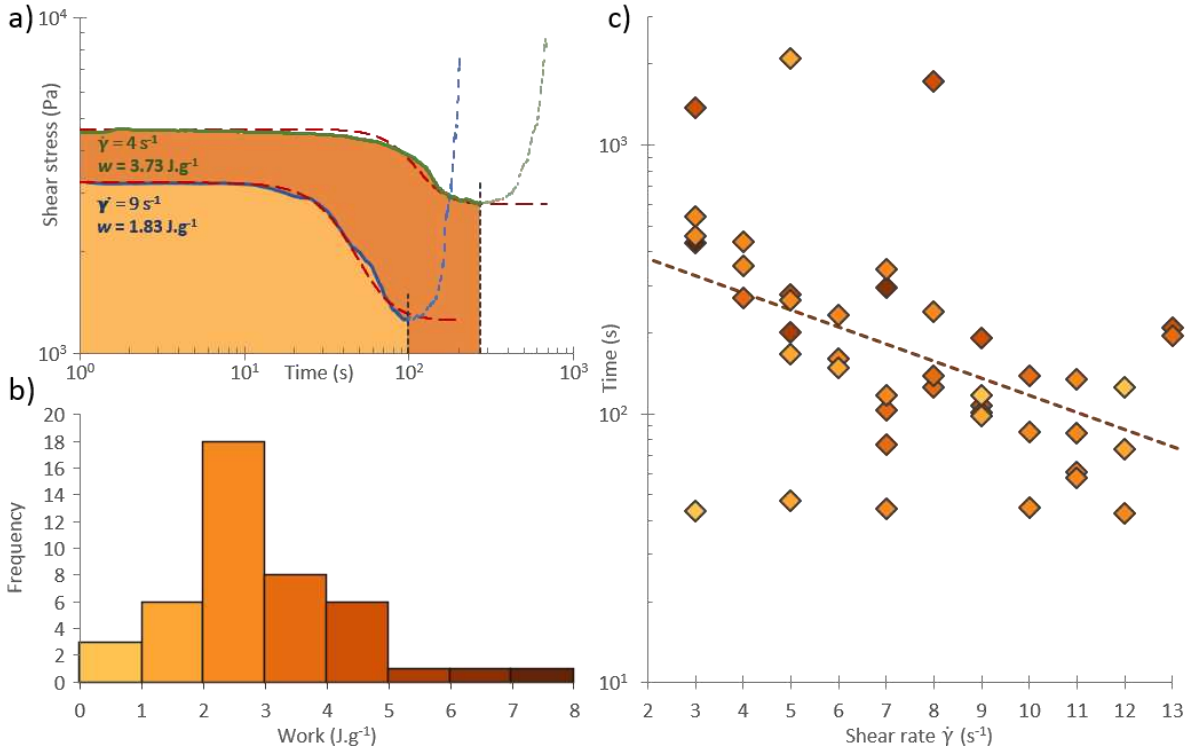

Figure 3 **– High rate steady shear responses. (a)** Two examples of fibroin's response to high rate steady shear are plotted. Both show the transition from a quasi-static viscosity to a lower plateau viscosity, after which a rapid increase in shear stress indicates sample gelation. The point at which gelation initiates is indicated, and forms the upper limit for the integrating beneath the curve using **Equation 4**. The total work done for each sample (Shaded areas) are grouped in **(b)**, with colours representing each $J.g^{-1}$ interval. **(c)** The relation between applied

shear rate and time to gelation is shown, with point coloured according to the total work done (see **(b)** for colour key).

This compares very favourably with our recent differential scanning calorimetry (DSC) measurements of thermal degradation of fibroin feedstocks (1.778±0.245 $J.g^{-1}$, n=27)[47] and supports the argument that silk solidification is best described in terms of total energetic input. Comparing our results with DSC data for other common model proteins such as albumen (17.0 $J.g^{-1}$),[48] we see that the minimum energetic input required for fibroin to undergo denaturation – defined as the energy required to first dehydrate and then subsequently alter the bonding confighuration in a protein[49–51] – is nearly an order of magnitude lower for both shear and heat-based energy inputs, which perfectly highlights the superb efficiency of silk based solidification.[44]

The slight difference between shear and heating energy input values becomes clear when the difference in end product is considered. In the DSC experiments, the end result is an amorphous isotropic mass formed through spontaneous denaturation of the fibroin solution. However, in the case of sheared samples, the end result is anisotropic, with alignment of structures across multiple length scales seen in the direction of shear.[44,45,52] This confirms that although silk gels incredibly easily, the generation of solid multiscale hierarchical structures (i.e. spinning a fibre) without premature gelation is a more energy intensive process – i.e. work must be done to align polymer chains, but at a rate low enough to avoid the spontaneous amorphous denaturation observed through calorimetry.

Perhaps at this juncture, most pertinent to the broader discussion is to question “what actually is a fibre?” Classical descriptions hold that they are simply long, slender objects which possess

sufficient flexibility to allow them to be woven into fabric, but we argue instead that, with the increased interest in biomimetic silk spinning, a stricter definition is required. While extruding protein solutions into a long, thin mass may have the macroscopic appearance of a fibre, and may represent promising advances in their respective fields, to call these short, stiff, or brittle protein extrudates fibres is perhaps misleading, unless they exhibit more of the interconnected hierarchical structural motifs present in natural silks.[1,53–55]

During the production of a natural silk fibre, silk protein feedstocks are converted into a solid through alignment, denaturation, crystallisation, aggregation and fibrillation (**Figure 4**). Therefore we suggest that natural silk production requires a controlled application of energy to facilitate this entire process over a specific timescale, first generating structures via intra then inter-protein interactions. Whilst it is evident that flow plays a key role in energy accumulation during natural spinning and is the animal's primary tool for generating precise structures in its materials, [2,12,56] this is in stark contrast to the current state of the art in artificial fibre production. Although alternative methods of energy application such as thermal or chemical approaches may seem more efficient or convenient, they may not facilitate structure development in a similar way, leading to products that do not exhibit all the traits of a natural silk fibre.[1]
^[1]^[1]^[1]^[1]^[1]We believe that the data presented herein offers a new window into artificial spinning, in that although silk will denature once a certain energetic threshold is passed, how that energy is supplied must be controlled in order to truly spin silk.

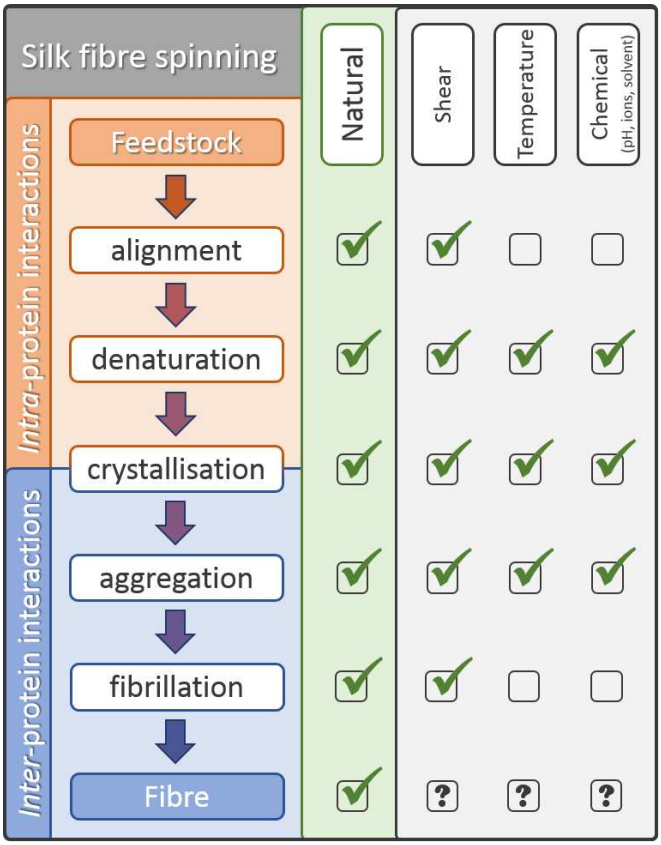

Figure 4 –Suggested comparative framework for silk fibre production. Whilst there are several means to solidify silk, not all are able to generate the hierarchical structures present in the final fibre.

4 Conclusions

Natural silk spinning is a process dependent on the careful application of energy to the feedstock through a combination of flow stresses, at different rates, for different time. Through a combination of steady shear experiments at a range of different shear rates, we present a map of the work required to induce solidifcation in the native silk feedstock from B. mori. By comparing our findings to calorimetry studies it is clear that there is an energy penalty associated with fibre formation that is not seen in other forms of feedstock solidification. This leads us to the proposition that not all solidfication routes are equal, causing us to reconsider what constitutes a natural silk fibre and the steps taken to produce it.

5 Supporting Information

Supporting Information is available from the Wiley Online Library or from the author.

6 Acknowledgements

This study was supported by the EPSRC (EP/K005693/1). This project has received funding from the European Union's Horizon 2020 research and innovation programme under grant agreement No 713475.

Received: Month XX, XXXX; Revised: Month XX, XXXX; Published online:

((For PPP, use "Accepted: Month XX, XXXX" instead of "Published online")); DOI: 10.1002/mabi.((insert number))

Keywords: silk spinning, Bombyx mori, rheology, fibroin, steady shear

7 References

1. A. Koeppel, C. Holland, ACS Biomater. Sci. Eng. **2017**, 3, 226.
2. J. Sparkes, C. Holland, Nat. Commun. **2017**, 8, 594.
3. C. L. Craig, Annu. Rev. Entomol. **1997**, 42, 231.
4. J. Sparkes, C. Holland, Acta Biomater. **2018**, 69, 234.
5. H. Kaneko, Bull. Chem. Soc. Jpn. **1934**, 9, 207.
6. H. Teramoto, T. Kameda, Y. Tamada, Biosci. Biotechnol. Biochem. **2008**, 72, 3189.
7. F. Chen, D. Porter, F. Vollrath, J. R. Soc. Interface **2012**, 9, 2299.
8. B. Mortimer, J. Guan, C. Holland, D. Porter, F. Vollrath, Acta Biomater. **2015**, 11, 247.
9. F. Vollrath, B. Madsen, Z. Shao, Proc. R. Soc. B Biol. Sci. **2001**, 268, 2339.
10. X. Liu, K. Zhang, Oligomerization Chem. Biol. Compd. **2014**, 69.
11. A. E. Brooks, S. R. Nelson, J. a. Jones, C. Koenig, M. B. Hinman, S. Stricker, R. V. Lewis, Nanotechnol. Sci. Appl. **2008**, 1, 9.
12. B. Mortimer, C. Holland, F. Vollrath, Biomacromolecules **2013**, 14, 3653.
13. M. B. Dickerson, P. B. Dennis, V. P. Tondiglia, L. J. Nadeau, K. M. Singh, L. F. Drummy, B. P. Partlow, D. P. Brown, F. G. Omenetto, D. L. Kaplan, R. R. Naik, ACS Biomater. Sci. Eng. **2017**, 3, 2064.
14. N. Dinjaski, D. Ebrahimi, S. Ling, S. Shah, M. J. Buehler, D. L. Kaplan, ACS Biomater. Sci. Eng. **2016**, acsbiomaterials.6b00236, doi:10.1021/acsbiomaterials.6b00236.
15. S. Lin, S. Ryu, O. Tokareva, G. Gronau, M. M. Jacobsen, W. Huang, D. J. Rizzo, D. Li, C. Staii, N. M. Pugno, J. Y. Wong, D. L. Kaplan, M. J. Buehler, Nat. Commun. **2015**, 6, 6892.
16. D. W. Kim, O. J. Lee, S.-W. Kim, C. S. Ki, J. R. Chao, H. Yoo, S. Yoon, J. E. Lee, Y. R. Park, H. Kweon, K. G. Lee, D. L. Kaplan, C. H. Park, Biomaterials **2015**, 70, 48.
17. H. Tao, B. Marelli, M. Yang, B. An, M. S. Onses, J. a. Rogers, D. L. Kaplan, F. G. Omenetto, Adv. Mater. **2015**, 27, 4273.
18. J. G. Hardy, S. a. Geissler, D. Aguilar, M. K. Villancio-Wolter, D. J. Mouser, R. C. Sukhavasi, R. C. Cornelison, L. W. Tien, R. C. Preda, R. S. Hayden, J. K. Chow, L. Nguy, D. L. Kaplan, C. E. Schmidt,

Macromol. Biosci. **2015**, 15, 1490.
19. H.-J. Jin, J. Park, R. Valluzzi, P. Cebe, D. L. Kaplan, Biomacromolecules **2004**, 5, 711.
20. A. Rising, Acta Univ. Agric. Sueciae **2007**.
21. N. Kronqvist, M. Sarr, A. Lindqvist, K. Nordling, M. Otikovs, L. Venturi, B. Pioselli, P. Purhonen, M. Landreh, H. Biverstål, Z. Toleikis, L. Sjöberg, C. V. Robinson, N. Pelizzi, H. Jörnvall, H. Hebert, K. Jaudzems, T. Curstedt, A. Rising, J. Johansson, Nat. Commun. **2017**, 8, 15504.
22. G. J. G. Davies, D. P. Knight, F. Vollrath, PLoS One **2013**, 8, e73225.
23. G. J. G. Davies, D. P. Knight, F. Vollrath, Tissue Cell **2013**, 45, 306.
24. M. Moriya, K. Ohgo, Y. Masubuchi, D. P. Knight, T. Asakura, Polymer (Guildf). **2008**, 49, 5665.
25. T. Asakura, J. Yao, M. Yang, Z. Zhu, H. Hirose, Polymer (Guildf). **2007**, 48, 2064.
26. T. Asakura, K. Umemura, Y. Nakazawa, H. Hirose, J. Higham, D. Knight, Biomacromolecules **2007**, 8, 175.
27. N. Kojic, M. Kojic, S. Gudlavalleti, G. McKinley, Biomacromolecules **2004**, 5, 1698.
28. J. Yao, H. Masuda, C. Zhao, T. Asakura, Macromolecules **2002**, 35, 6.
29. F. Zhang, Q. Lu, X. Yue, B. Zuo, M. Qin, F. Li, D. L. Kaplan, X. Zhang, Acta Biomater. **2015**, 12, 139.
30. P. Corsini, J. Perez-Rigueiro, G. V. Guinea, G. R. Plaza, M. Elices, E. Marsano, M. M. Carnasciali, G. Freddi, J. Polym. Sci. Part B Polym. Phys. **2007**, 45, 2568.
31. C. Holland, A. E. Terry, D. Porter, F. Vollrath, Nat. Mater. **2006**, 5, 870.
32. C. Holland, A. E. Terry, D. Porter, F. Vollrath, Polymer (Guildf). **2007**, 48, 3388.
33. C. Holland, D. Porter, F. Vollrath, Biopolymers **2012**, 97, 362.
34. P. R. Laity, S. E. Gilks, C. Holland, Polymer (Guildf). **2015**, 67, 28.
35. P. R. Laity, C. Holland, Biomacromolecules **2016**, 17, 2662.
36. P. R. Laity, C. Holland, Int. J. Mol. Sci. **2016**, 17, 1812.
37. P. R. Laity, E. Baldwin, C. Holland, Macromol. Biosci. **2018**, 1800188, doi:10.1002/mabi.201800188.
38. H. Janeschitz-Kriegl, E. Ratajski, M. Stadlbauer, Rheol. Acta **2003**, 42, 355.
39. O. O. Mykhaylyk, P. Chambon, R. S. Graham, J. P. A. Fairclough, P. D. Olmsted, A. J. Ryan, Macromolecules **2008**, 41, 1901.
40. O. O. Mykhaylyk, P. Chambon, C. Impradice, J. P. A. Fairclough, N. J. Terrill, A. J. Ryan, Macromolecules **2010**, 43, 2389.
41. P. R. Laity, L. Baldwin, C. Holland, **2018**.
42. W. P. Cox, E. H. Merz, J. Polym. Sci. **1958**, 28, 619.
43. M. P. Escudier, I. W. Gouldson, A. S. Pereira, F. T. Pinho, R. J. Poole, J. Nonnewton. Fluid Mech. **2001**, 97, 99.
44. C. Holland, F. Vollrath, A. J. Ryan, O. O. Mykhaylyk, Adv. Mater. **2012**, 24, 105.
45. C. Holland, J. S. Urbach, D. L. Blair, Soft Matter **2012**, 8, 2590.
46. M. Moriya, K. Ohgo, Y. Masubuchi, T. Asakura, Polymer (Guildf). **2008**, 49, 952.
47. C. Holland, N. A. Hawkins, M. Frydrych, P. R. Laity, D. Porter, F. Vollrath, Unpublished **2018**.
48. J. W. Donovan, C. J. Mapes, J. G. Davis, J. A. Garibaldi, J. Sci. Food Agric. **1975**, 26, 73.
49. D. Porter, F. Vollrath, Soft Matter **2008**, 4, 326.
50. D. Porter, F. Vollrath, Biochim. Biophys. Acta - Proteins Proteomics **2012**, 1824, 785.
51. D. Porter, F. Vollrath, Soft Matter **2013**, 9, 643.
52. M. Boulet-Audet, A. E. Terry, F. Vollrath, C. Holland, Acta Biomater. **2014**, 10, 776.
53. M. Andersson, J. Johansson, A. Rising, Int. J. Mol. Sci. **2016**, 17, 1290.
54. A. Leal-Egaña, T. Scheibel, Biotechnol. Appl. Biochem. **2010**, 55, 155.
55. D. Ebrahimi, O. Tokareva, N. G. Rim, J. Y. Wong, D. L. Kaplan, M. J. Buehler, ACS Biomater. Sci. Eng. **2015**, 1, 864.
56. D. P. Knight, F. Vollrath, Proc. R. Soc. London **1999**, 266, 519.

8 TOC entry

Rheology unravels the energetic requirements for the spinning of silk fibres. This study uses rheological data to calculate the energy input required to solidify a silk under flow, which can be used to guide the future development of truly biomimetic spinning devices.

J. Sparkes, C. Holland*

The energy requirements for flow induced solidification of silk

9 Supporting Information

for Macromol. Biosci., DOI: 10.1002/mabi.2013#####

The energy requirements for flow induced solidification of silk

J. Sparkes, C. Holland*

9.1 Note 1

Perhaps the most startling contribution from this experiment is the time required to reach equilibrium under steady shear, with length scales far in excess of that assumed in typical shear rate ramps, meaning that there is a far greater dependence on rates of change than previously assumed, and suggests that prior attempts to describe the shear-thinning behaviour of fibroin feedstocks using, for example, the CY model, may also be under-representative of the true steady state viscosity of a given feedstock. However, the alternative, which involves subjecting samples to a stepped shear rate with step lengths longer than the expected equilibration time, is unlikely to prove more worthy across a useful range of rates, since the total work accumulation in the sample under such a test is likely to exceed the point of denaturation itself, thus rendering a sample void before complete mapping of the regime is achieved.

9.2 Figure S1

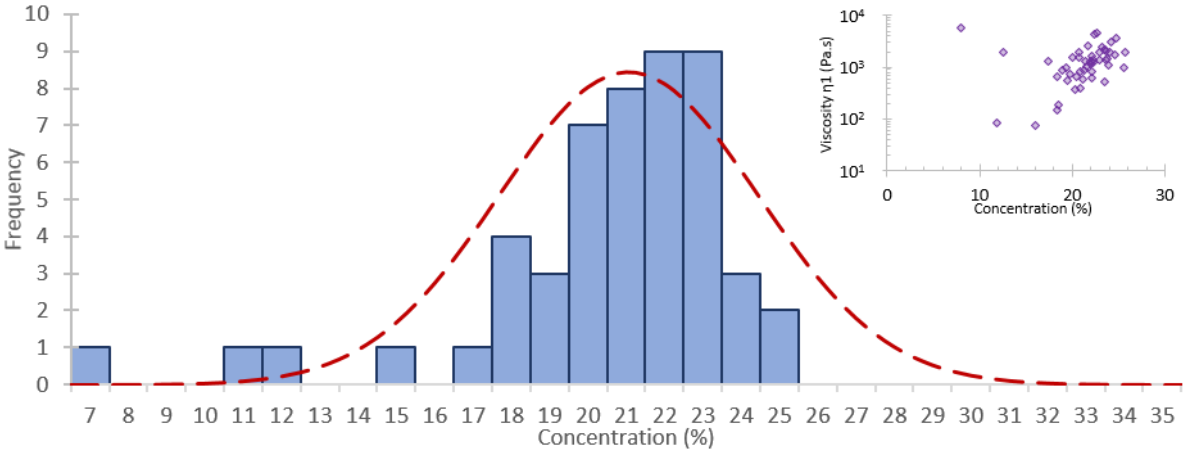

Figure 5 - Fibroin Concentration: determined as a dry weight fraction is 21.7 ± 5.5% (n=50), comparable to previous studies describing fibroin concentration[34]. **(Inset) The viscosity-concentration relation:** Little relation is seen, with a wide range of viscosities present for a given concentration.

9.3 Figure S2

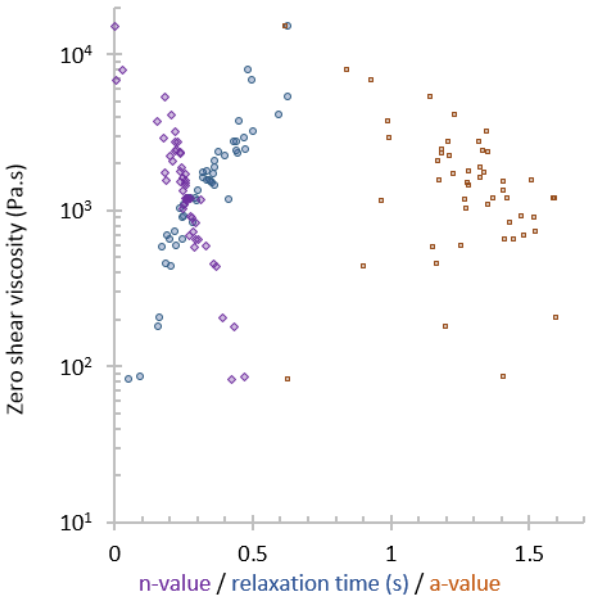

Figure 6 Relation between simplified Carreau-Yasuda model parameters fitted to Oscillatory data via the Cox-Merz relation.